DIODE-LASER SPECTROSCOPY OF ALKALI HALIDES:
THE SODIUM FLUORIDE MOLECULE

M.C. DOUAY [1], A.M.R.P. BOPEGEDERA, C.R. BRAZIER and P.F. BERNATH [2]

Department of Chemistry, University of Arizona, Tucson, AZ 85721, USA

The vibration–rotation spectrum of the sodium fluoride molecule was recorded using a diode laser. A total of 127 rotational lines were recorded in the first overtone band (2–0) and several hot bands with $\Delta v = 2$. These data, combined with previous microwave measurements, enabled us to determine ten vibration–rotation constants for NaF including $\omega_e = 535.6594(15)$ cm^{-1} and $\omega_e x_e = 3.57636(68)$ cm^{-1}.

1. Introduction

The alkali halide molecules are prototypical models for ionic bonding and occur commonly in flames. As a result of this interest, these molecules have been studied by many different techniques ranging from microwave spectroscopy [1] to photoelectron spectroscopy [2]. However, there are few high-resolution infrared observations. We report here on the vibration–rotation spectrum of NaF obtained by diode laser spectroscopy.

High-resolution infrared spectra are available for the lithium halides, LiF [3], LiCl [4,5], LiBr [6] and LiI [7] as well as KF [8]. For NaF, low-resolution gas phase observations [9] and matrix isolation measurements are published [10–12]. The infrared matrix isolation spectra of $(NaF)_x$ dimers and polymers were also studied [12,13].

The rotational constants of NaF are known with great precision from the millimeter measurements of Veazey and Gordy [14] and from microwave measurements [15,16]. The radio frequency and microwave work [15,16] also established the dipole moment of NaF (8.156 D for $v=0$) and provided values for additional constants such as the electric

quadrupole hyperfine coupling parameters.

The properties of the NaF molecule have been calculated by ab initio [17–19] and semi-empirical quantum chemical methods [20]. The empirical Rittner model [21] and variations on this theme [22–27] provides surprisingly accurate representations of the ground state potential energy curve.

The ultraviolet absorption and emission spectra of alkali halides are called the "fluctuation bands" [28,29]. They are largely of a bound–free nature, therefore little spectroscopic information can be extracted. Photofragmentation spectroscopy (see, for example, ref. [30]) does provide some information on the excited state potential energy curves and the dissociation energy.

The study of alkali halides in hydrogen–oxygen–nitrogen flames gives estimates of the dissociation energies (121 kcal/mol for NaF) [31]. A chemiluminescent flame resulting from the combustion of alkali metal fuels with halogen oxidisers can also provide estimates for the dissociation energy [32]. The pioneering work of M. Polanyi [33] on metal-halogen flames continues to provide inspiration [34,35].

2. Experimental

NaF vapor was generated in a stainless steel heat pipe oven. This was a 1 m long, 50 mm diameter tube

[1] Current address: Laboratoire de Spectroscopie des Molécules Diatomiques, Université des Sciences et Techniques de Lille, Bâtiment P5, 99655 Villeneuve d'Ascq Cedex, France.
[2] Alfred P. Sloan Fellow; Camille and Henry Dreyfus Teacher-Scholar.

equipped with BaF_2 windows and electrically heated over the center 0.6 m section. The ends of the tube were water cooled to confine the alkali halide vapor to the central part of the tube. Approximately 50 g of NaF (Aldrich) was placed on a stainless wire mesh inside the tube and the cell was pressurized with about 2 Torr of argon, which acts as a buffer gas to maintain the NaF vapor in the central part of the cell. The cell was heated to about 1000°C to obtain a reasonable concentration (≈ 100 mTorr) of the NaF vapor resulting in up to 1% absorption. The sample could be heated many times over a period of two weeks without recharging the cell with NaF.

A Pb–Sn–Te diode laser (Laser Analytics) was used to record several $\Delta v = 2$ vibration–rotation bands of the NaF molecule. The laser beam was passed eight times through the cell providing an effective path length of about 4 m through the NaF vapor. A 0.33 m monochromator was used to select a single longitudinal mode of the laser. The laser beam was then imaged on to a liquid-N_2-cooled Hg–Cd–Te detector. The laser diode was frequency modulated at approximately 4 kHz and the NaF absorption lines were detected using a lock-in amplifier at twice the modulation frequency. Absolute frequency calibration of the lines was provided by placing a 0.2

m cell containing 0.5 Torr of NH_3 in the beam path and comparing with the published spectrum of $^{14}NH_3$ and $^{15}NH_3$ (in natural abundance) [36]. A small portion of the beam was passed through an air-spaced germanium Fabry–Perot etalon with a free spectral range of 0.029851 cm^{-1} to provide relative frequency calibration.

The absorption signal (NaF and NH_3) and the etalon signal were recorded simultaneously on a two-pen chart recorder. The position of the unblended rotational lines could be determined with an accuracy of about ± 0.002 cm^{-1}.

3. Results and discussion

A total of 127 rotational lines in the first overtone, 2–0, and the hot bands 3–1, 4–2, 5–3, 6–4, 7–5, 8–6 of the Na–F stretch were recorded in this experiment. The absorption of the fundamental band 1–0, and the hot bands with $\Delta v = 1$ are stronger than that of the overtone bands with $\Delta v = 2$ but we had no diodes in this spectral region. Initiallly the millimeter wave data reported by Veazey and Gordy [14] and the infrared data reported by Ritchie and Lew [9] were used to predict the rotational line positions
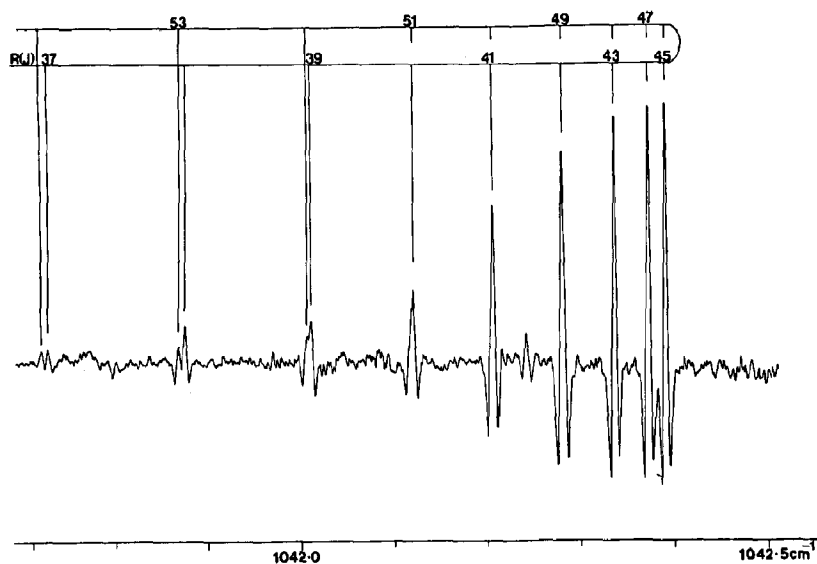

Fig. 1. The 4–2 band of X $^1\Sigma^+$ state of NaF. Note that near the band head the low J rotational lines going into the band head and the high J lines coming out of the band head are accidentally overlapped. The relative intensities of the lines are distorted by the variation of the diode laser power.

Table 1
Rotational line positions of the $\Delta v=2$ transitions of NaF (in cm^{-1})

R(J)	2–0 band		3–1 band		4–2 band		6–4 band		8–6 band	
	ν	$10^3\Delta\nu$	ν	$10^3\Delta\nu$	ν	$10^3\Delta\nu$	ν	$10^3\Delta\nu$	ν	$10^3\Delta\nu$
6			1041.807	−1						
30	1068.062	−1								
31	1068.344	−1					1013.428	2		
32			1054.551	−1			1013.682	3		
33			1054.790	−4			1013.916	2		
34			1055.021	3			1014.133	2		
35			1055.227	4	1041.377	−1	1014.335	5		
36			1055.415	6	1041.557	−6	1014.518	7	988.289	2
37	1069.649	4	1055.583	6	1041.728	−1	1014.681	7	988.440	−8
38	1069.798	2	1055.730	3	1041.875	−2	1014.817	−2	988.583	−8
39	1069.929	1	1055.854	−3	1042.010	4	1014.945	−1	988.719	3
40	1070.038	−3	1055.965	−4	1042.120	3	1015.052	−3	988.826	2
41	1070.130	−6	1056.061	−2	1042.206	−3	1015.146	0	988.916	3
42	1070.205	−6	1056.137	−1	1042.281	−2	1015.219	0	988.992	7
43	1070.264	−4	1056.193	−1	1042.336	−3	1015.269	−4	989.041	2
44	1070.302	−4	1056.230	−1	1042.371	−4	1015.309	−1	989.078	2
45	1070.321	−4	1056.249	0	1042.389	−5	1015.326	−2	989.086	−9
46	1070.321	−3	1056.249	1	1042.389	−4	1015.326	−2	989.086	−9
47	1070.302	−3	1056.230	1	1042.371	−3	1015.309	−1	989.079	0
48	1070.265	−2	1056.193	1	1042.336	−1	1015.269	−4	989.044	−0
49	1070.205	−5	1056.137	2	1042.281	0	1015.219	0	988.996	4
50	1070.130	−4	1056.061	2	1042.206	0	1015.146	0	988.921	−0
51	1070.038	−1	1055.965	0	1042.120	7	1015.052	−3	988.832	−1
52	1069.924	−0	1055.854	2	1042.006	6	1014.945	−1	988.725	−2
53	1069.791	−0	1055.722	2	1041.868	−2	1014.817	−1	988.592	−11
54	1069.640	1	1055.574	5	1041.722	2	1014.681	9	988.449	−13
55			1055.405	6	1041.549	−3	1014.518	10	988.249	−8
56			1055.214	4	1041.367	2	1014.331	6		
57			1055.004	1			1014.126	1		
58			1054.773	−3			1013.909	4		
59			1054.530	−1			1013.671	3		
60	1068.319	−5					1013.415	3		
61	1068.033	−5								
P(9)	1041.681	−1								

of the 2–0 band. The 2–0 band was then recorded and the above prediction was used in making the rotational assignments. We found that near the band head, the low J rotational lines going into the band head and the higher J lines coming out of the band head were accidentally overlapped. This blending was observed in all of the bands that were recorded (fig. 1). The rotational line positions of the 2–0 band and the millimeter wave data [14] were then fitted to the Dunham energy level expression [37]

$$E_{vJ} = \sum_{kj} Y_{kj}(v+\tfrac{1}{2})^k[J(J+1)]^j.$$

The improved molecular constants obtained from this fit were then used to predict the rotational line positions of the 3–1 band, which was recorded and subsequently fitted. By this repeated process of prediction, recording and fitting, we were able to make the rotational assignments of the measured lines reported in table 1. The rotational line positions of the 5–3 band could not be measured since it was obscured by the presence of what we believe to be a combination band of the sodium fluoride dimer [12,13,38]. The 7–5 band of NaF is in a region where there are no NH$_3$ calibration lines thus these rota-

Table 2
Dunham vibration–rotation constants for the NaF molecule in the $X\,^1\Sigma^+$ state (in cm^{-1})

Y_{10}	535.6594(15)[a]	Y_{01}	0.43690108(12)
Y_{20}	−3.57636(68)	$10^3 Y_{11}$	−4.55801(21)
$10^2 Y_{30}$	1.878(11)	$10^5 Y_{21}$	2.3006(98)
$10^5 Y_{40}$	−8.55(64)	$10^8 Y_{31}$	3.7(11)
		$10^6 Y_{02}$	−1.16349(47)
		$10^9 Y_{12}$	5.491(50)

[a] One standard deviation error in parentheses.

tional lines were not measured. For the final fit all of the lines reported in table 1 were fitted together with the three microwave transitions [15] and the ten millimeter wave transitions to obtain the vibration–rotation constants of the NaF molecule reported in table 2.

These vibration–rotation constants were then used as input for an RKR program to obtain the potential curve for the $X\,^1\Sigma^+$ ground state of the NaF molecule. The classical turning points thus obtained are given in table 3. The equilibrium bond length was calculated to be 1.925 94 Å. The turning points reported in table 3 were used to plot the potential energy curve for the NaF molecule (fig. 2). This potential energy curve is quite harmonic with the outer curve extending to larger r very slowly with the increasing vibrational quantum number. This is to be expected as the molecule has a dissociation energy $D_0^0 = 40\,300\ cm^{-1}$ [19] and the levels probed range only up to 4300 cm^{-1}, about 10% of the well depth.

The hot bands 3–1, 4–2 and 5–3 are stronger than the 2–0 band despite the fact that the population falls by about a factor of two for each successive vibra-
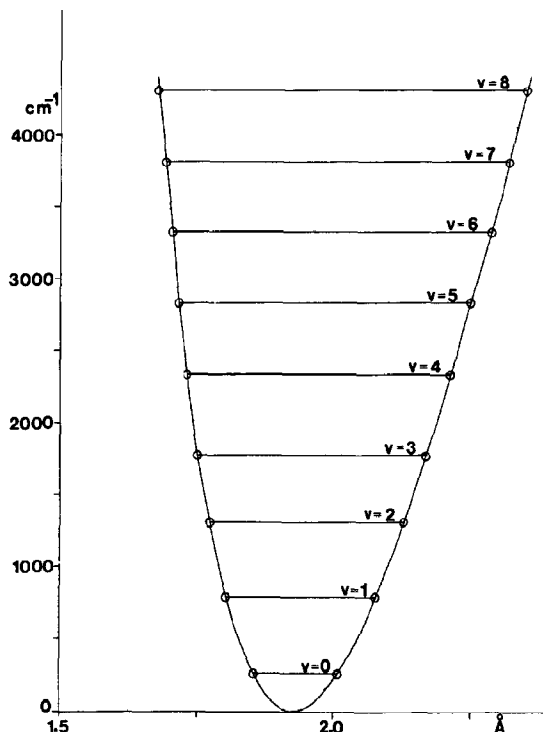

Fig. 2. The potential energy curve for the $X\,^1\Sigma^+$ ground state of NaF. The equilibrium constants reported in table 2 were used to calculate the RKR potential curve.

tional level. This indicates that the vibrational transition dipole strength increases rapidly with vibration quantum number. For bands with v'' greater than 3, the absorption decreases as the effect of decreasing population overcomes the increase in transition strength.

Acknowledgement

Table 3
RKR turning points of the potential energy curve of the $X\,^1\Sigma^+$ state of NaF

v	E_v (cm^{-1})	R_{min} (Å)	R_{max} (Å)
0	267.1152	1.85284	2.00890
1	795.6825	1.80490	2.07665
2	1317.2635	1.77436	2.12712
3	1831.9668	1.75093	2.17062
4	2339.8991	1.73161	2.21013
5	2841.1650	1.71506	2.24699
6	3335.8670	1.70052	2.28197
7	3824.1055	1.68752	2.31553
8	4305.9788	1.67575	2.34798

References

[1] A. Honig, M. Mandel, M.L. Stich and C.H. Townes, Phys. Rev. 96 (1954) 629.
[2] T.D. Goodman, J.D. Allen Jr., L.C. Cusachs and G.K. Schweitzer, J. Electron Spectry. 3 (1974) 289.

[3] A.G. Maki, J. Mol. Spectry. 102 (1983) 361.

[4] H. Jones and J. Lindenmayer, Chem. Phys. Letters 135 (1987) 189.

[5] G.A. Thompson, A.G. Maki, W.B. Olson and A. Weber, J. Mol. Spectry. 124 (1987) 130.

[6] C.R. Brazier, N.H. Oliphant and P.F. Bernath, in preparation.

[7] G. Thompson, A.G. Maki and A. Weber, J. Mol. Spectry. 118 (1986) 540.

[8] A.G. Maki and F.J. Lovas, J. Mol. Spectry. 95 (1982) 80.

[9] R.K. Ritchie and H. Lew, Can. J. Phys. 42 (1964) 43.

[10] A. Snelson and K.S. Pitzer, J. Phys. Chem. 67 (1963) 882.

[11] V.I. Baikov and K.P. Vasilevskii, Opt. Spectry. 22 (1967) 198.

[12] T.P. Martin and H. Schaber, J. Chem. Phys. 68 (1978) 4299.

[13] Z.K. Ismail, R.H. Hauge and J.L. Margrave, J. Inorg. Nucl. Chem. 35 (1973) 3201.

[14] S.E. Veazey and W. Gordy, Phys. Rev. 138A (1965) 1303.

[15] R.K. Bauer and H. Lew, Can. J. Phys. 41 (1963) 1461; 42 (1964) 830.

[16] C.D. Hollowell, A.J. Hebert and K. Street Jr., J. Chem. Phys. 41 (1964) 3540.

[17] P.K. Swaninathan and E. Clementi, J. Phys. Chem. 91 (1987) 1020.

[18] P. Pyykkö, G.H.F. Diercksen, F. Müller-Plathe and L. Laaksonen, Chem. Phys. Letters 141 (1987) 535.

[19] S.R. Langhoff, C.W. Bauschlicher Jr. and H. Partridge, J. Chem. Phys. 84 (1986) 1687.

[20] Y. Zeiri and G.G. Balint-Kurti, J. Mol. Spectry. 99 (1983) 1.

[21] E.S. Rittner, J. Chem. Phys. 19 (1951) 1030.

[22] P. Brumer and M. Karplus, J. Chem. Phys. 58 (1973) 3903.

[23] J. Shanker, H.B. Agrawal and G.G. Agrawal, J. Chem. Phys. 73 (1980) 4056.

[24] M. Kumar, A.J. Kaur and J. Shanker, J. Chem. Phys. 84 (1986) 5735.

[25] J. Shanker and H.B. Agrawal, Can. J. Phys. 58 (1980) 950.

[26] B.T. Gowda and S.W. Benson, J. Phys. Chem. 86 (1982) 847.

[27] J.E. Szymanski and J.A.D. Matthew, Can. J. Phys. 62 (1984) 583.

[28] R.F. Barrow and A.D. Caunt, Proc. Roy. Soc. A 219 (1953) 120.

[29] P. Davidovits and D.C. Brodhead, J. Chem. Phys. 46 (1967) 2968.

[30] T.R. Su and S.J. Riley, J. Chem. Phys. 72 (1980) 6632.

[31] E.M. Bulewicz, L.F. Phillips and T.M. Sugden, Trans. Faraday Soc. 57 (1961) 921.

[32] D.O. Ham, J. Chem. Phys. 60 (1974) 1802.

[33] M. Polanyi, Atomic reactions (Williams and Norgate, London, 1932).

[34] P. Arrowsmith, S.H.P. Bly, P.E. Charters and J.C. Polanyi, J. Chem. Phys. 79 (1983) 283.

[35] P. Davidovitz and D.L. McFadden, Alkali halide vapors (Academic Press, New York, 1979).

[36] G. Guelachvilli and K. Narahari Rao, Handbook of infrared standards (Academic Press, Orlando, 1986).

[37] J.L. Dunham, Phys. Rev. 41 (1932) 721.

[38] M. Eisenstadt, G.M. Rothberg and P. Kusch, J. Chem. Phys. 29 (1958) 797.